

## INVESTIGATING THE STEADY STATE MODE OF POWER INVERTERS FOR INDUCTION HEATING

**Evgeniy Popov, Nikolay Hinov**

Faculty of Electronic Engineering and Technologies, Department of Power Electronics,  
Technical University of Sofia, Sofia, Bulgaria

**Abstract.** *This article formulates the new unified interpretation of the analysis of electromagnetic processes in the autonomous (usually resonant) inverters with power circuits having a serial RLC configuration either with or without free wheeling diodes. The investigation starts with clarifying the parameters of the inverter circuit by bringing the fourth order power network into such of a second order in a normalized form. On this basis the novel compendious relationships between the most important internal inverter parameters are given. A MATLAB program calculates and displays the frequency characteristics of both types of inverters and simulates their steady state. The results from characteristics and simulation confirm each other in many ways. They were also proved experimentally. The whole processed information helps better understanding and organizing intelligent design, measurement and control of the inverters for technological applications (induction heating).*

**Key words:** *modeling, electromagnetic processes, frequency characteristics, RLC inverters, steady state, unified interpretation.*

### 1. INTRODUCTION

The voltage fed RLC inverter (Fig. 1), its dual counterpart the current fed RLC inverter and the serial RLC inverter without free-wheeling diodes (Fig. 2) cover a very wide range of practical autonomous inverter circuits generally applied in electronic technology [1]-[4]. In this case important and complex mutually connected problems are the accurate design of the power circuit, appropriate adjustment between the inverter and the load and adequate control providing stable, reliable and efficient operation of the converter when wide variations of the load are expected [5]-[7].

The mathematical relationships between the parameters of the mentioned inverters are rather complicated [5], [8]-[10]. It has been proved that all the quantities in these second order

---

Received September 15, 2016; received in revised form September 29, 2017

**Corresponding author:** Nikolay Hinov

Faculty of Electronic Engineering and Technologies, Department of Power Electronics, Technical University of Sofia, Sofia, Bulgaria

(E-mail: hinov@tu-sofia.bg)

topologies depend on two variables - the ratio between the controlling angular frequency and the generalized angular frequency (frequency coefficient)  $n_{\omega 1} = n_{\omega} = \omega / \Omega$  on one hand, and the ratio between the damping coefficient and the generalized angular frequency  $n_{\delta 1} = n_{\delta} = \delta / \Omega$  of the power circuit, on the other. At the same time engineering practice in the area of the power electronics needs fast and accurate means for simultaneous solution of the already stated problems.

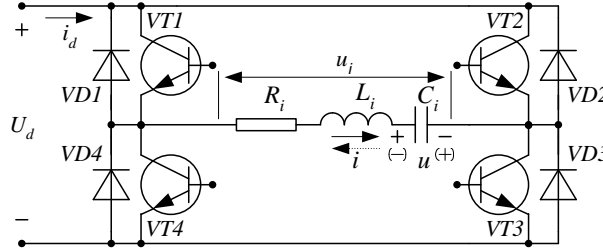


**Fig. 1** Voltage fed RLC inverter

When, for oscillatory mode  $R_i < 2\sqrt{L_i / C_i}$  of the inverter circuit (Fig 1, Fig. 2) coefficient is  $c = 1$ , for over damped mode ( $R_i > 2\sqrt{L_i / C_i}$ )  $c = -1$  and for critical mode ( $R_i = 2\sqrt{L_i / C_i}$ )  $c = 0$ .

The parameters that determine the development of the electromagnetic processes in the steady state in the power inverter circuits are

$$n_{\delta 1} = n_{\delta} = \frac{\delta}{\Omega} = \frac{B_I \cos \phi_I}{\sqrt{c(4B_I \sin \phi_I - B_I^2 \cos^2 \phi_I)}} \text{ (osc.; over damped); } 1 \text{ (critical)} \quad (1)$$

For resonant inverters (oscillatory mode) the coefficient of hesitation is

$$k_I = 1 / [1 - \exp(-\pi \delta / \omega_0)] = 1 / [1 - \exp(-\pi n_{\delta})] \quad (2)$$

The frequency coefficient is

$$n_{\omega 1} = n_{\omega} = \frac{\omega}{\Omega} = \frac{2}{\sqrt{c(4B_I \sin \phi_I - B_I^2 \cos^2 \phi_I)}} \text{ (osc.; over damped); } \frac{2}{B_I \cos \phi_I} \text{ (critical)} \quad (3)$$

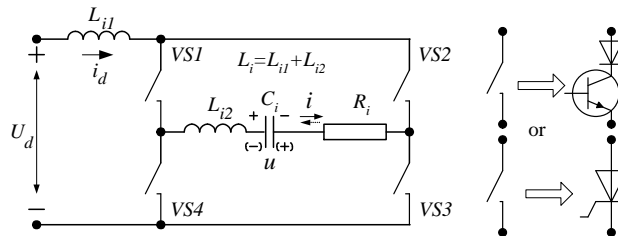


**Fig. 2** A serial RLC inverter without free-wheeling diodes

## 2. THE INVERTER ANALYSIS IN THE STEADY STATE MODE

In contrast to the approaches used in [10]-[15] provided herein is a unified approach to the analysis, which alleviates the description of the behavior of the power circuit. A constant  $c_i$  reflecting the type of the inverter is introduced, having values  $c_i = +1$  for the RLC inverter with free wheeling diodes (Fig. 1) or  $c_i = -1$  for the RLC inverter without free wheeling diodes (Fig. 2).

The following designations are applied:  $f_s(x) = \sin x$ ,  $f_c(x) = \cos x$ ,  $\delta = R_i / (2L_i)$ ,  $\Omega = \omega_0 = \sqrt{1/(L_i C_i) - \delta^2}$  for oscillatory mode;  $f_s(x) = \sinh x$ ,  $f_c(x) = \cosh x$ ,  $\delta = R_i / (2L_i)$ ,  $\Omega = \sqrt{\delta^2 - 1/(L_i C_i)}$  for over damped mode;  $f_s(x) = x$ ,  $f_c(x) = 1$ ,  $\delta = R_i / (2L_i)$ ,  $\Omega = \delta$  for critical mode.

Then the inverter current and the voltage across the capacitor  $C_i$  can be written in the following manner

$$i = \frac{U_d + U_0}{\Omega L} e^{-\delta t} f_s(\Omega t) - c_i I_0 e^{-\delta t} \left[ f_c(\Omega t) - \frac{\delta}{\Omega} f_s(\Omega t) \right] \quad (4)$$

$$u = U_d - (U_d + U_0) e^{-\delta t} \left[ f_c(\Omega t) + \frac{\delta}{\Omega} f_s(\Omega t) \right] - c_i \frac{I_0}{\Omega C} e^{-\delta t} f_s(\Omega t) \quad (5)$$

The angle  $\theta_2 = \theta_0 = \pi \Omega / \omega = \pi / n_\omega$  corresponding to the half period is determined from the controlling angular frequency  $\omega = 2\pi f$  and the generalized frequency  $\Omega$ .

The parameters of the inverter circuit (Fig. 1, Fig. 2) can be determined taking into account the initial conditions for the steady state

$$\begin{aligned} i(0) &= -c_i i(\theta_0) \\ u(0) &= -u(\theta_2) \end{aligned} \quad (6)$$

and

$$i(\theta_1) = 0 \quad (7)$$

Then the determination of the parameters follows. The parameter  $a = I_0 \Omega L / (U_d + U_0)$  is

$$a = \frac{f_s(\theta_2)}{e^{n_\delta \theta_2} + c_i f_c(\theta_2) - c_i n_\delta f_s(\theta_2)} \quad (8)$$

For the inverter in Fig. 1 only the angle  $\theta_1$  is determined from

$$\frac{f_s(\theta_1) / f_c(\theta_1)}{1 - n_\delta f_s(\theta_1) / f_c(\theta_1)} = a \quad (9)$$

The generalized coefficient of hesitation is

$$K = \frac{1}{1 + e^{-n_\delta \theta_2} [(c_i c a + n_\delta + c_i a n_\delta^2) f_s(\theta_2) + f_c(\theta_2)]} \quad (10)$$

It should be underlined that when calculating  $a$  and  $K$  for discontinuous inverter current mode for Fig. 2  $\theta_0 = \theta_2$  must be equal to  $\pi$  in the already given expressions (8) and (10).

The initial capacitor voltage is

$$U'_0 = \frac{U_0}{U_d} = 2K - 1 \quad (11)$$

The maximal voltage across the capacitor  $C_i$   $U'_m$  for Fig. 2 is also given by (11). For Fig. 1 it is given by

$$U'_m = \frac{U_m}{U_d} = 2\left(\frac{K}{K_i} - K\right) - 1 \quad (12)$$

The expression for the coefficient  $K_1$  is the same as (10), but the variable  $\theta_2$  is exchanged with  $\theta_1$  ( $\theta_2 \rightarrow \theta_1$ ).

The normalized inverter current and capacitor voltage are respectively

$$i'(\theta) = \frac{i(\theta)\Omega L}{U_d} = 2Ke^{-n_s\theta} \left[ (1 + c_i a n_s) f_s(\theta) - c_i a f_c(\theta) \right] \quad (13)$$

$$u'(\theta) = \frac{u(\theta)}{U_d} = 1 - 2Ke^{-n_s\theta} \left[ (c_i c a + n_s + c_i a n_s^2) f_s(\theta) + f_c(\theta) \right] \quad (14)$$

The average value of the input current (all values are normalized) is

$$I'_d = \frac{I_d \Omega L}{U_d} = \frac{1}{\theta_0} \int_0^{\theta_0} i'(\theta) d\theta = \frac{1}{\theta_0} \cdot \frac{2(2K-1)}{n_s^2 + c} \quad (15)$$

The RMS value of the inverter current is

$$I' = I\Omega L / U_d = \sqrt{I'^2 / (2n_s)} \quad (16)$$

The output characteristic (Fig. 1 and Fig. 2) is

$$OCH = I' / I'_d \quad (17)$$

The input characteristic is

$$ICH = 1 / (n_\omega I'_d) \quad (18)$$

The characteristic of the coefficient of nonlinear distortion (klir – factor) of the inverter current is

$$kf[\%] = 100 \cdot \sqrt{I'^2 - I'_{(1)}^2} / I'_{(1)} \quad (19),$$

where  $I'(m)$  ( $m = 1, 3, 5, 7, \dots$ ) is the  $m$ -th harmonic component of the inverter current. (The mathematical expressions for calculation of the harmonic components in the different circuits and modes of operation are disparate, and rather complicated. They have been found and published in earlier authors' publications.)

From that point on the analysis of the power inverter may be continued without problems in a normalized or in a non normalized form.

3. AN EXAMPLE WITH A SERIAL RESONANT INVERTER WITHOUT FREE WHEELING DIODES

A half bridge circuit (Fig. 3) is under study but it can be easily converted into the bridge one. The power losses in the inverter are neglected. The commutation of the power semiconductor devices is instantaneous. A parallel equivalent circuit represents the induction heater. The quality factor of the load circuit is sufficiently high that the voltage across the load has a close to the sine wave shape.

A MATLAB program processes all the mathematical information describing the steady state operation of the inverter in the allowed frequency range. The frequency characteristics of the inverter are obtained and graphically displayed in Fig. 4. These particular characteristics correspond to a practically implemented inverter (PT1-100-2400) with the following data:  $U_d=500\text{ V}$ ;  $L_K=45\ \mu\text{H}$ ;  $C_K=84\ \mu\text{F}$ ;  $R_l=0.4739599\ \Omega$ ,  $f_{lr}=2083\text{ Hz}$ ,  $L_{lr}=8.8717\ \mu\text{H}$ ,  $C_b=657.88\ \mu\text{F}$ ,  $n_1=0$ ,  $n_2=1$ ,  $f=1600\text{ -}2600\text{ Hz}$ . The first graphic shows: the average input current  $I_d$  [A] (solid line). The second graphic shows: the maximal device voltage  $U_{Vsm}$  (solid line). Other parameters of the circuit can also be calculated and displayed.

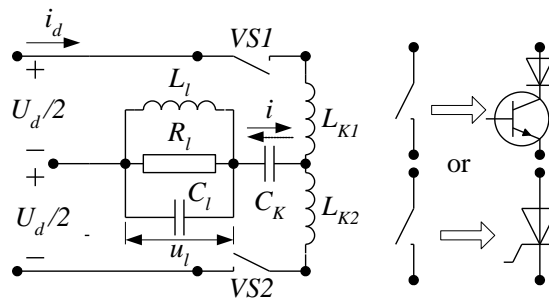


Fig. 3 A practical serial resonant inverter without free-wheeling diodes

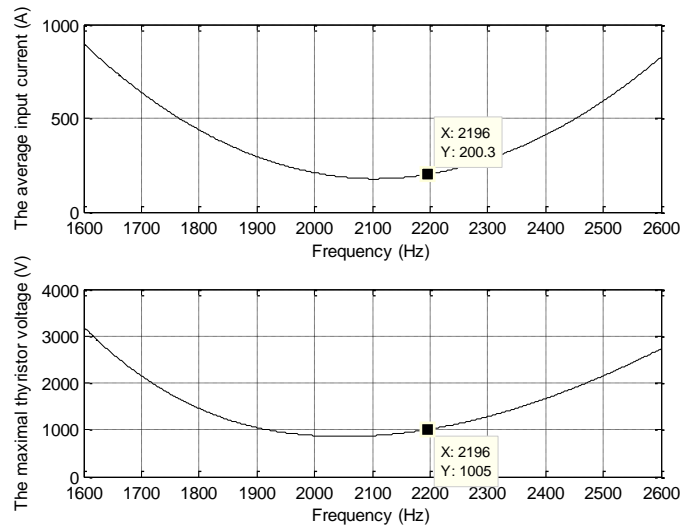
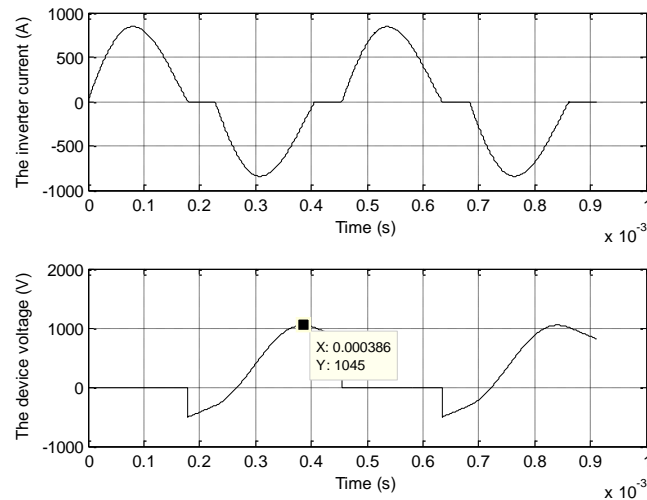


Fig. 4 The inverter frequency characteristics

The stability and efficiency of the inverter can be studied from the characteristics. In general there is a minimum of the input current and power, load voltage, serial capacitor voltage and device voltage around the resonance of the load circuit. If the parameters of the inductor heater vary during the induction heating process it is advisable to maintain almost constant input current (power) in a slight capacitive detuning of the load circuit  $R_l, L_l, C_l$ , where the operation is stable, by exercising an influence on the controlling frequency. The calculated slope of the frequency characteristic of the input current helps for determining the parameters of the closed loop automatic control system.



**Fig. 5** The detailed simulation results at  $f = 2195$  Hz

The steady state is simulated by a MATLAB program based on the method described in [16] for direct determination of the steady state mode (in the case for the discontinuous inverter current mode) that is experimentally confirmed. The results from the frequency characteristics, from the simulation and from *experiments* are in good agreement according to Table I. That confirms the correctness of the whole study. The detailed simulation results of the power inverter are graphically displayed (Fig. 5) for  $f=2195$  Hz. The first diagram shows: the inverter current  $i_{CK}$  [A] (solid line). The second diagram shows: the voltage across a device  $u_{VSI}$  [V] (solid line). The simulation results for the same circuit at  $f=694$  Hz displaying an interesting case – a non typical but possible operation in an inductive detuning of the load generally with the third harmonic component of the inverter current (a case that is difficult to be studied analytically) are given in Fig. 6.

**Table 1** Results for fig. 3

f[Hz]	694		1823			2018		2083
Study	Sim.	Fr.ch.	Sim.	Fr.ch.	<i>Exper.</i>	Sim.	Fr.ch.	
Load	Ind.		Ind.			Ind.	<b>Res.</b>	
$I_d$ [A]	169.5	400.7	388.7	200	200	196.5	178.2	
$U_l$ [V]	200.4	304.4	303.5	215.4	217	215.8	201.7	
$t_{q.c.}$ [μS]	604	113.6	125.9	61	65	68.3	63.8	
$U_{CKm}$ [V]	1456	1308	1270	590	585	580	509	
$U_{VSm}$ [V]	1927	1342	1342	866	870	875	863	

f[Hz]	2083	Recom.		2195		2394	
Study	Sim.	<b>Fr.ch.</b>	<i>Exper.</i>	<b>Sim.</b>	Fr.ch.	Sim.	
Load	Res.			<b>Cap.</b>		Cap	
$I_d$ [A]	180.1	<b>199.8</b>	<i>200</i>	<b>208.2</b>	400.6	416.3	
$U_l$ [V]	206.6	<b>211.9</b>	<i>218</i>	<b>222.1</b>	302.2	314.1	
$t_{q.c.}$ [μS]	72.5	<b>82.9</b>	<i>85</i>	<b>89.9</b>	97.3	99.6	
$U_{CKm}$ [V]	515	<b>542</b>	<i>560</i>	<b>565</b>	996	1034	
$U_{VSm}$ [V]	886	<b>1003</b>	<i>1030</i>	<b>1045</b>	1636	1689	

#### 4. AN EXAMPLE WITH A SERIAL RESONANT INVERTER WITH FREE WHEELING DIODES

A real circuit is given in Fig. 7. The inverter frequency characteristics are graphically displayed in Fig. 8. They correspond to an inverter (PT2-50-4000) with:  $U_d=500$  V;  $L_K=0.3$  mH;  $C_K=4$  μF;  $R_r=4$  Ω;  $f_r=4000$  Hz,  $\cos\phi_r=0.24254$ ,  $n_1=0$ ,  $n_2=1$ ,  $f=3000 - 4800$  Hz. The graphics show: the average input current  $I_d$  [A] (solid line); the load voltage  $U_{Lm}$  [V] (solid line). For each frequency there is a check whether the shape of the load voltage is close to the sine wave.

The increase of the controlling frequency leads to increase of the input current (power), load voltage, peak serial capacitor voltage and RMS value of the inverter current and to decrease of the circuit turn-off time. But around the load resonant frequency the character of most functions is opposite (inflexed points) and the changes of parameters are not so large. Therefore, if the load  $R_b, L_l$  varies during the induction heating, it is advisable to maintain a resonance of the load circuit  $R_b, L_l, C_l$  by influencing the controlling frequency. The results from the frequency characteristics, from the simulation of the steady state mode and from *experiments* are compared in Table 2. They are in good agreement confirming the correctness of the results.

The steady state results for  $f=4000$  Hz are shown in Fig. 8. They are:  $i_{CK}$  [A] (solid line),  $u_1$  [V] (solid line).

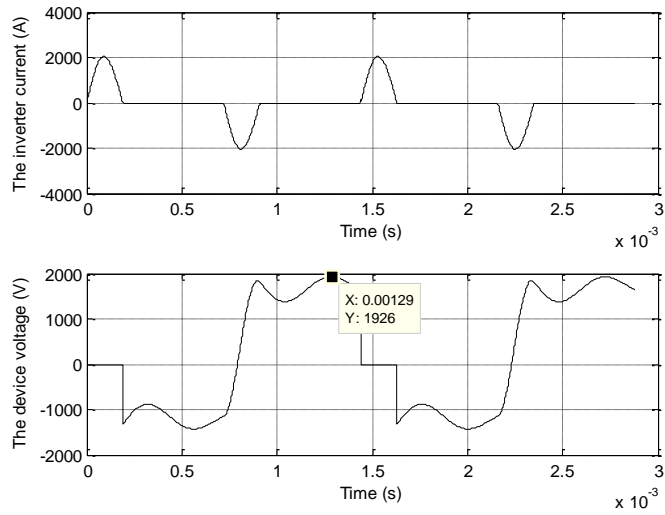


**Fig. 6** The detailed simulation results for  $f = 694$  Hz

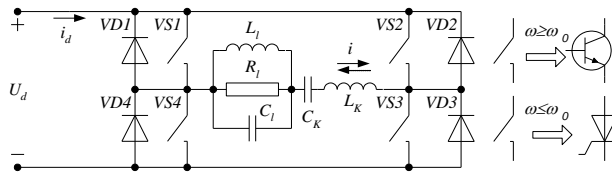


**Fig. 7** A real resonant inverter with free-wheeling diodes

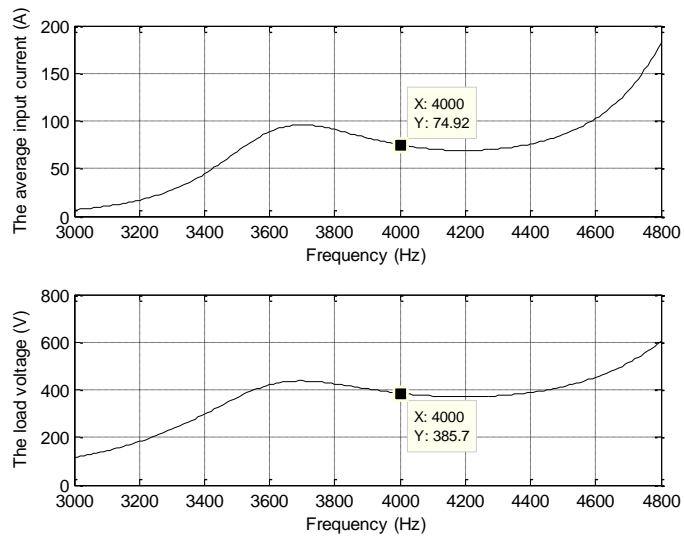


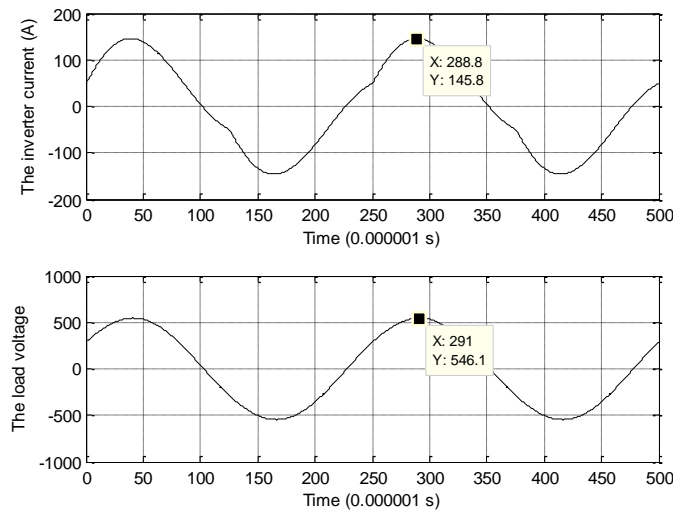
**Fig. 8** The inverter frequency characteristics



**Table 2** Results for Fig. 8

Par.	Hz	f= 3200		f= 3600		Recom.	f= 4000	
		Fr.ch.	Sim.	Fr.ch.	Sim.		Fr.ch.	Exper.
$I_d$ ,A		16.74	16.62	88.53	88.39	<b>74.92</b>	<b>75</b>	<b>74.34</b>
$V_1$ ,V		182.3	182.3	420.2	420.5	<b>385.7</b>	<b>387</b>	<b>385.6</b>
$t_{q,c}$ , $\mu$ S.		69.83	70.31	35.98	36.88	<b>22.33</b>	<b>22</b>	<b>23.19</b>
$V_{CKm}$ ,V		1683	1700	2129	2125	<b>1320</b>	<b>1325</b>	<b>1320</b>
$I_{CK}$ ,A		94.20	94.58	137.7	137.8	<b>96.77</b>	<b>97</b>	<b>96.75</b>

Par.	Hz	f = 4400		f= 4800	
		Fr.ch.	Sim.	Fr.ch.	Sim.
$I_d$ ,A		75.81	75.45	182.0	181.7
$V_1$ ,V		388.7	388.5	603.1	602.8
$t_{q,c}$ , $\mu$ S.		31.13	31.31	24.28	24.42
$V_{CSm}$ ,V		1548	1551	3120	3121
$I_S$ ,A		122	122	268	268

**Fig. 9** The detailed simulation results at  $f = 4000$  Hz

## 5. CONCLUSIONS

Serial RLC inverters with or without free wheeling diodes for induction heating are investigated. A novel unified interpretation of the electromagnetic processes is applied based on the previously calculated inverter network parameters in a normalized form. The frequency characteristics, the steady state simulation parameters and the *experimental* results are obtained and mutually confirmed. That proves the correctness of the whole study. The requirements for the control system are defined, which is useful for research on the type of offline simulation, hardware in the loop and rapid prototyping. The main contribution of the work is an approach to analysis of series RLC DC/AC converters for

induction heating. This allows the creation of methods for engineering design that are simple, such as mathematical ones, but with sufficient precision for engineering practice.

#### REFERENCES

- [1] B. L. Dokić, B. Blanuša, *Power Electronics Converters and Regulators* - Third Edition, © Springer International Publishing, Switzerland 2015, ISBN 978-3-319-09401-4.
- [2] E. I. Berkovitch, G. V. Ivenskiy, Yu. S. Yoffe, A. T. Matchak, V. V. Morgun, *Higher frequency thyristor converters for electro technological units*, St. Petersburg, Energoatomizdat, (1973), 1983, (In Russian).
- [3] M. K. Kazimierczuk and D. Czarkowski, *Resonant Power Converters*, IEEE Press and John Wiley & Sons, New York, NY 2nd Edition, pp. 1-595, ISBN 978-0-470-90538-8, 2011.
- [4] N. Mohan, Undeland, M. Tore, William P. Robbins, *Power Electronics - Converters, Applications, and Design* (3rd Edition), © 2003 John Wiley & Sons.
- [5] A. Dominguez, A. Otin, L. A. Barragan, J. I. Artigas, D. Navarro, and I. Urriza, "Frequency-to-output-power transfer function measurement of a resonant inverter for domestic induction heating applications", In Proceedings of the IEEE Annual Conference of the Industrial Electronics Society IECON13, Vienna, Austria, 2013, pp. 5032-5037
- [6] E. Popov, *Analysis, Modeling and Design of Converter Units (Computer – Aided Design of Power Electronic Circuits)*, Technical University Printing House, Sofia, 2005 (In Bulg.), Chapters 2-3, pp. 59–80.
- [7] O. Lucía, P. Maussion, E. Dede, and J. M. Burdío, "Induction heating technology and its applications: Past Developments, current technology, and future challenges", *IEEE Transactions on Industrial Electronics*, vol. 61, pp. 2509-2520, May 2014.
- [8] A. Dominguez, L. Barragan, J. Artigas, A. Otin, I. Urriza, D. Navarro, "Reduced-order Models of Series Resonant Inverters in Induction Heating Applications", *IEEE Transactions on Power Electronics*, vol. 32, Issue: 3, pp. 2300 – 2311, March 2017.
- [9] A. Dominguez, L. A. Barragan, J. I. Artigas, A. Otin, I. Urriza, and D. Navarro, "Reduced-order model of a half-bridge series resonant inverter for power control in domestic induction heating applications", In Proceedings of the IEEE International Conference on Industrial Technology (ICIT), 2015, pp. 2542-2547.
- [10] Y. Yin, R. Zane, R. Erickson, and J. Glaser, "Direct modelling of envelope dynamics in resonant inverters", *Electronics Letters*, vol. 40, pp. 834-836, 2004.
- [11] D. Maksimovic, A. M. Stankovic, V. J. Thottuvelil, and G. C. Verghese, "Modeling and simulation of power electronic converters", In Proceedings of the IEEE, 2001, vol. 89, pp. 898-912.
- [12] F. H. Dupont, C. Rech, R. Gules, and J. R. Pinheiro, "Reduced-Order Model and Control Approach for the Boost Converter With a Voltage Multiplier Cell", *IEEE Transactions on Power Electronics*, vol. 28, pp. 3395-3404, 2013.
- [13] J. Sun and H. Grotstollen, "Averaged modeling and analysis of resonant converters," In Proceedings of the 24th Annual IEEE of the Specialists Conference on Power Electronics PESC '93, 1993, pp. 707-713.
- [14] S. Tian, F. C. Lee, and Q. Li, "A Simplified Equivalent Circuit Model of Series Resonant Converter" *IEEE Transactions on Power Electronics*, vol. 31, pp. 3922-3931, 2016.
- [15] Y. Yan, R. Zane, R. Erickson, and J. Glaser, "Direct modeling of envelope dynamics in resonant inverters", In Proceedings of the 34th Annual IEEE Conference on Power Electronics Electronic PESC '03, 2003, 2003, vol.3, pp. 1313-1318.
- [16] E. I. Popov, "Direct determination of the steady-state mode in autonomous inverters", *Scientific Journal Electrical Engineering and Electronics E+E*, Sofia, Bulgaria, (In Bulg.), vol. 11-12, 2004.